International Journal for Multidisciplinary Research (IJFMR)
E-ISSN: 2582-2160 ● Website: www.ijfmr.com ● Email: editor@ijfmr.com

Exploring Aspartate Semialdehyde Dehydrogenase as a Prospective Drug Target for Fungal Pathogens: An Extensive Molecular Modeling Studies

Swathi Nataraj[1], Shristi Saini[1,2], Oruganti Amsu Madhu Deepika[1], Lakshminarayanan Karthik[1]

[1]Precision Therapeutics Laboratory, Quick IsCool, Aitele Research LLP, Bihar, India.
[2]Molecular Oncology, Department of Biochemistry, University of Lucknow, India.

Abstract
Trichophyton rubrum (T. rubrum) and Blastomyces dermatitidis (B. dermatitidis) are two fungal species that pose significant threats to human health. T. rubrum is a dermatophyte fungus that causes athlete's foot, fungal nail infections, and jock itch, and the ringworm B. dermatitidis is a dimorphic fungus that causes blastomycosis. Aspartate semialdehyde dehydrogenase (ASADH) is an enzyme that catalyzes the reductive dephosphorylation of β-aspartyl phosphate to L-aspartate-β-semialdehyde in the aspartate biosynthetic pathway of plants and microorganisms. The inhibition of ASADH has resulted in a substantial reduction in the populations of several pathogenic microbial organisms. An extensive literature review revealed that ASADH could be considered a promising drug target for identifying and developing compounds with potent antifungal activity. Therefore, in the present study, a comprehensive in silico screening of compound libraries was initially carried out to identify possible ASADH inhibitors. The chosen drug targets (ASADH from T. rubrum and B. dermatitidis) were subsequently subjected to molecular docking with those chemical libraries via PyRx. The results revealed that in each library, a subset of potential small molecules exhibited higher binding affinities for T. rubrum and B. dermatitidis's ASADH. In addition, analysis of their physicochemical and ADMET properties confirmed that several of the higher-ranked compounds exhibited drug-likeness properties. Taken together, our findings show that the compounds identified in the present study open new avenues for drug development, and further in vitro and in vivo validation studies are needed to assess their efficacy and safety profiles for the development of novel antifungal treatments.

Keywords: Aspartate semialdehyde dehydrogenase, Trichophyton rubrum, Blastomyces dermatitidis, In silico, Virtual screening docking, ADMET analysis

Introduction

Fungi are more challenging to treat without damaging the host because eukaryotic animal cells and fungal cells share many of the same basic cell structures and machinery [1]. Fungal infections, commonly known as mycosis, can affect any part of the human body. They can appear on several parts

of the body: on the surface of the skin, nails, or mucous membranes (superficial or mucocutaneous), underneath the skin (subcutaneous), or inside other organs of the body, such as the lungs, brain, or heart (deep infection). Fungal infections occur when one type of fungal microbe becomes too prevalent in one area of the body so that the immune system cannot overcome it. The skin, mucosal membranes, white blood cells, antibodies, etc., prevent fungal organisms from spreading and causing invasive infections. However, it has been estimated that fungal diseases affect more than 1.5 million people, where the severity of occurrence ranges from non-symptomatic, subtle mucocutaneous infections to severe systemic infections [2].

T. rubrum is a dermatophytic fungus that survives on skin surfaces. It was first described by Castellani in 1910 as tinea cruris and was first named *Epidermatophyton rubrum* [3]. Dermatophytes (or dermatomycetes) can enter the keratin-rich tissues of humans as well as various animals, causing dermatophytosis (or dermatomycosis) [4]. The fungus is responsible for nail, hair follicle, and superficial skin infections. In rare cases, it can cause a puss or swollen area in the deeper skin layers or even affect and spread to internal organs, including the brain, liver, muscle, and bone [5]. An anthropophilic dermatophyte, these fungi are also known to spread infection to healthy individuals through contact with infected persons' hair or skin, which is commonly found on clothing, combs, socks, and towels [6]. *T. rubrum* can live for up to 12 months inside humans; therefore, it is easily transmitted from person to person. These infections are more common in hot weather because of excessive perspiration and friction in the intertriginous area. Symptoms of Trichophyton infection include patches of hair loss, scaly rash, scaling on the scalp, and itching, producing blister-like lesions such as subcutaneous abscess, fistula, nodules, granuloma, and folliculitis [7].

B. dermatitidis is another fungus that was reported by T. C. Gilchrist in 1894 and assumed that the infection was caused by a protozoan. However, after working with W.R. Stokes, Gilchrist isolated the organism and termed it *B. dermatitidis* [8]. This dimorphic fungus causes blastomycosis, also known as Gilchrist's disease, in humans and other animals after they inhale the microscopic fungal spores from the air [9]. The fungal spores cannot be observed with the naked eye because of their size. Blastomyces adhesin1 (BAD1) is an important virulence protein that enhances Blastomyces adhesion to host cells, inhibits immune cell activation, and represses the production of TNF-α, a cytokine that helps in the host defence mechanism [10,11]. This yeast can stay in the lungs or move through the bloodstream to the brain, stomach, intestine, and skin, with the skin remaining the most preferred site for infection. Blastomycosis can also be transmitted through needlestick injuries and animal bites [12]. Diagnosing this fungal infection can be challenging due to its ability to resemble lung cancer, skin cancer, tuberculosis, nocardiosis and several other granulomatous disorders, and the symptoms range from asymptomatic infection to severe multiorgan system involvement [13].

ASADH is an enzyme that plays a crucial role in the production of amino acids, which include lysine and methionine in prokaryotes, fungi, and some higher plants, as well as the cell wall component diaminopimate from aspartate. This enzyme is also involved in sporulation in gram-negative bacteria. It catalyzes the reductive dephosphorylation of β-aspartyl phosphate to L-aspartate-β-semialdehyde in the aspartate biosynthesis pathway of plants and microorganisms [14,15]. As mammals, including humans, lack ASADH or its homologue and do not rely on the aspartate biosynthetic pathway, this enzyme is often considered an attractive target for developing novel antifungal compounds [16]. Furthermore, because ASADH is known to contribute to the production of approximately 25% of critical amino acids in these pathogens [17], the present study has attempted to target ASADH from both *T. rubrum* and *B.*

dermatitidis through molecular docking studies. By utilizing various computational methods, such as compound-based library screening, virtual screening docking and physicochemical and pharmacokinetics analysis, the findings of this study establish the groundwork for developing potent antifungal compounds that target ASADH.

Materials and Methods

Protein Preparation

The crystal structures of the drug targets ASADH from *T. rubrum* (PDB: 4ZHS) and *B. dermatitidis* (PDB: 6C85) were retrieved from the Protein Data Bank. The cocrystal ligands in these two protein structures were permanently deleted before virtual screening docking was initiated. In addition, polar hydrogens were added to the protein structures, and Kohlman charges were assigned to the atoms that constitute the protein. This phase is critical because it ensures the exact representation of electrostatic interactions throughout the docking procedure. Following this, any water molecules, co-crystallized ligands or usual artifacts found in protein structures were eliminated. This technique is commonly used to speed up the docking process and reduce computing complexity.

Selection of Compound Libraries - Ellagic Acid

Several studies have shown that plant extracts can serve as a potential source for novel antifungal agents, offering an alternative to synthetic drugs given their noteworthy pharmacological and toxicological attributes [18,19]. Ellagic acid, a phenolic compound that is abundant in numerous plants, is widely recognized for its antioxidant, antibacterial, and antiulcerogenic properties. Interestingly, its antifungal effects have not been previously documented [20]. Neves and colleagues conducted a study that revealed that the ethanol extract of ellagic acid exhibited a strong affinity for the enzyme ASADH from *T. rubrum*, thus underscoring its antifungal activity among various phenolic compounds [19].

IMB-XMA0038

IMB-XMA0038 is a center-stage inhibitor that is specifically designed to target ASADH in fungal pathogens. Its unique mode of action involves binding to the enzyme, disrupting its activity and impeding the production of key amino acids necessary for fungal survival. This disruption inhibits the growth and proliferation of fungal pathogens, suggesting a new approach to combat these infections [21].

2-Chloro-3-Methoxy-1,4-Naphthoquinone

The biosynthetic pathways for amino acids in the aspartate family share common initial steps that convert oxaloacetate into l-aspartate and subsequently into l-homoserine in a series of three consecutive reactions. These pathways involve complex interactions and have been the subject of extensive investigation as potential sources for new antifungal targets [22,23]. The initial step in the biosynthesis of aspartate family amino acids is facilitated by ASADH, which is encoded by the HOM2 gene. Deleting this gene, which is responsible for encoding ASADH, has been shown to result in growth defects in bacteria. A recent study investigated ASADH inhibitors derived from p-benzoquinone, where one particular compound, 2-chloro-3-methoxy-1,4-naphthoquinone, effectively inhibited ASADH in *Cryptococcus neoformans*, *Candida albicans*, *Aspergillus fumigatus*, and *B. dermatitidis*, with Ki values ranging from 0.88 to 2.5 μM [24].

Hence, for the present study, the above-mentioned three compounds, “Ellagic acid," "IMB-XMA0038," and "2-chloro-3-methoxy-1,4-naphthoquinone," were selected as the lead compounds (Figure 1). The PubChem and binding databases were subsequently searched for small-molecule compounds that share structural similarities with the selected lead compounds. Among those repositories, a considerable number of hits, i.e., compound that satisfied Lipinski's rule of five and shared structural similarities with the lead compounds were retrieved in 3-D format from the PubChem database.

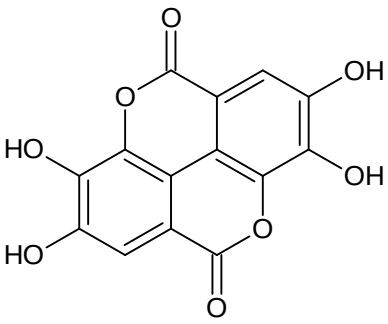

Ellagic Acid
(PubChem Id: 5281855)

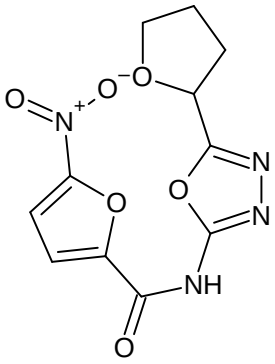

IMB-XMA0038
(PubChem Id: 44030060)

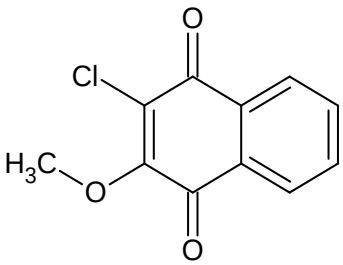

2-chloro-3-methoxy-1,4-naphthoquinone
(PubChem Id: 27459)

Figure 1: 2D Chemical Diagrams of the Selected Lead Compounds

Molecular Docking using PyRx

The virtual screening docking process was executed via AutoDock Vina, which was incorporated into PyRx version 0.8 [25]. AutoDock Vina is a widely utilized molecular docking tool employed to predict how ligands bind to receptors or proteins. The 3D structures of the chosen lead compound libraries were retrieved from PubChem in "sdf" format and subsequently converted to “pdbqt" files via Open Babel, an integrated component of PyRx software. To facilitate molecular docking, a three-dimensional grid box was established, configured with an exhaustiveness setting of eight. This configuration allows the program to systematically explore numerous ligand conformations in search of the best docking position with a high level of precision. The box dimensions were as follows: for the target protein (PDB: 4ZHS): size_x = -55.444 Å; size_y = 50.4955 Å; size_z = 9.1779 Å, yielding an XYZ dimension of 54 × 57× 55 Å; and for the target protein (PDB: 6C85): size_x = -55.401 Å; size_y = 50.1948 Å; size_z = 9.4229 Å, yielding an XYZ dimension of 142 × 149 × 150 Å. During the docking process, the ligands were allowed to adapt their conformations for optimal binding. In contrast, proteins are treated as rigid structures, maintaining their fixed conformation. The outcomes of the interactions between the target protein and ligands during docking were subsequently analyzed and visualized (data not shown) using Chimera X software [26] and the Discovery Studio program [27].

SwissADME Evaluation of Physicochemical Parameters

The evaluation of the physicochemical and ADMET (absorption, distribution, metabolism, excretion, and toxicology) properties of specific lead compounds when new medications are developed is a method used to mitigate potential adverse effects associated with treatments. This approach can reduce overall costs by eliminating molecules with inadequate ADMET properties from the drug development pipeline.

Accordingly, in the present study, a thorough assessment of the physicochemical and ADMET qualities of the higher-ranking compounds was performed via two prominent online platforms: SwissADME [28] for physicochemical analysis and pkCSM [29] for ADMET prediction. Both platforms provide an understanding of the characteristics of the lead compounds. SwissADME specifically evaluates factors related to a molecule's physicochemical properties, including size, weight, solubility, and acidity; pharmacokinetic properties, which refer to how the body absorbs, distributes, metabolizes, and excretes the molecule; drug likeliness, which reflects the similarity of the molecule to existing drugs; and medical chemistry friendliness, which reflects the ease of its synthesis in the laboratory setting. SwissADME helps to identify promising drug candidates by evaluating their suitability for further development.

pkCSM Evaluation of ADME Properties and Toxicity Predictions

Eventually, pkCSM specifically evaluates pharmacokinetic properties, which refer to the processes of absorption through the gut wall, distribution throughout the body, metabolism by enzymes, excretion of a drug through urine or feces in the body, and toxicity properties of the molecule, including AMES mutagenicity tests, acute and chronic toxicity in rats, skin sensitization, and organ toxicity. pkCSM is a valuable tool that can anticipate early-stage drug discovery through *in silico* assessment.

Results

The docking score is the scoring function used to predict the binding affinity of both the ligand and target once they are docked. The higher the binding energy is, the stronger the predicted binding affinity between the ligand and the protein. In the present study, the top-ranked compounds from the chosen libraries docked against *T. rubrum's* ASADH exhibited binding energies ranging from "-10.4 to -6.6 kcal/mol" (Table 1a). Similarly, the higher-ranked compounds identified from the same set of libraries and docked against *B. dermatitidis's* ASADH demonstrated binding energies within the range of "-8.8 to -7.3 kcal/mol" (Table 1b). In addition, the target enzymes were also tested against several known antifungal drugs. For example, compounds such as “terbinafine,” “moniconazole,” and “clotrimazole” were screened against *T. rubrum's* ASADH, whereas “itraconazole” and “amphotericin B” were docked against *B. dermatitidis's* ASADH. The results clearly showed that the binding energy of these existing drugs was relatively lower than that of the lead compounds presented in Table 1a and comparable to that of the lead compounds presented in Table 1b. Collectively, the molecular docking studies confirmed that the lead compounds identified from the three libraries possess promising binding affinities toward ASADH (from *T. rubrum* and *B. dermatitidis*), indicating their potential as drug candidates for further development in the treatment of antifungal infections.

Table 1a: Virtual screening docking of lead compounds against ASADH from *T. rubrum* (PDB: 4ZHS)

Sl. No	Ellagic Acid Library	Binding Energy (kcal/mol)	IMB-XMA0038 Library	Binding Energy (kcal/mol)	2-Chloro-3-methoxy-1,4-naphthoquinone Library	Binding Energy (kcal/mol)	Control Drugs	Binding Energy (kcal/mol)
1	11294619	-10.4	7267137	-8.7	164517454	-8.9	Terbinafine	-6.6
2	9101645	-10.0	7655523	-8.6	11211153	-7.7	Miconazol	-6.5

	5						e	
3	11290032	-9.6	7244049	-8.5	158303463	-6.7	Clotrimazole	-6.4
4	90785191	-9.3	7655527	-8.4	20165701	-6.7		
5	145980140	-9.3	2168077	-8.4	276680	-6.7		
6	145658936	-9.3	1356738	-8.3	13887390	-6.6		
7	166479754	-9.3	678894	-8.3	164517453	-6.6		
8	143180720	-9.1	4130759	-8.2	164517455	-6.6		
9	5488919	-8.9	959022	-8.2	275103	-6.6		
10	53946689	-8.6	7686800	-8.1	54283595	-6.6		

Table 1b: Virtual screening docking of lead compounds against ASADH from *B. dermatitidis* (PDB: 6C85)

Sl. No	Ellagic Acid Library	Binding Energy (kcal/mol)	IMB-XMA0038 Library	Binding Energy (kcal/mol)	2-Chloro-3-methoxy-1,4-naphthoquinone Library	Binding Energy (kcal/mol)	Control Drugs	Binding Energy (kcal/mol)
1	11294619	-8.8	12440425	-8.3	72792957	-7.9	Itraconazole	-8.2
2	70681273	-8.4	2104531	-8.2	19872801	-7.7	Amphotericin B	-8.2
3	5491816	-8.3	7244049	-8.1	158303463	-7.6		
4	56676784	-8.3	12549487	-8.0	164517454	-7.6		
5	91016455	-8.1	2104545	-8.0	10945787	-7.5		
6	123263024	-7.8	45809809	-7.9	19873044	-7.4		
7	91112913	-7.6	2739411	-7.9	54283595	-7.4		
8	91157994	-7.5	844311	-7.9	11211153	-7.4		
9	53946689	-7.4	25818784	-7.8	19872848	-7.3		
10	59184440	-7.3	7655523	-7.8	19872838	-7.3		

Physicochemical and Drug Likeness Properties

The physicochemical properties are the physical and chemical properties, which include the molecular weight of the drug molecule, its solubility, ionization state and its hydrogen-bonding capacity. According to Lipinski's rule of five, for an ideal drug compound, the molecular weight (MW) must be less than (or equal to) 500 g/mol, no more than 5 hydrogen bond donors (HBDs), no more than 10 hydrogen bond acceptors (HBAs) and a topographical polar surface area (TPSA) of no more than 140 $Å^2$. The log $P_{o/w}$ (consensus) is the average of all five lipophilic predictions (iLOGP, XLOGP3, WLOGP, MLOGP, and SILICOS-IT), where an oral drug with a LogP value of less than 5 is considered good for oral and intestinal absorption. The log S (ESOL) model predicts the aqueous solubility of a compound directly from its structure, whose acceptable range is between -4 and 6. Bioavailability is a term used to describe the percentage of an administered dose of a xenobiotic that reaches the systemic circulation. A bioavailability score of less than or equal to 0.55 is considered ideal. Veber's rule further increases the criteria for bioavailability with fewer than 10 rotatable bonds and a polar surface area (PSA) no greater than 140. The Ghose filter attempts to improve the prediction by stating that high absorption is likely if the following criteria are met: MW of 160 to 480 Da, LogP of -0.4 to 5.6, a molar refractivity of 40 to 130, and a total number of atoms between 20 to 70. The Egan rule considers good bioavailability for compounds with a TPSA ≤ 132 $Å^2$ and a LogP of ≥ -1 to ≤ 6. Muegge's rule changed the property ranges for parameters such as MW (200–600 Da), LogP (-2–5), PSA ≤ 150, number of rings ≤ 7, number of carbons > 4, number of heteroatoms > 1, and rotatable bonds ≤ 15 to differentiate between drug-like and nondrug-like compounds.

Table 2a: Physicochemical Property Analyses of the Ellagic Acid Library (PDB: 4ZHS)

Sl. No	Compound ID	Mol. wt g/mol	HBA	HBD	TPSA ($Å^2$)	Log $P_{o/w}$ (Consensus)	Log S (ESOL)	Drug likeness: Y(Yes)/N(No) (Lipinski Rules)	Bioavailability
1	11294619	482.44	8	2	119.34	4.18	-6.00	Y, 0 Violation	0.55
2	91016455	448.34	10	4	167.64	2.45	-4.70	Y, 0 Violation	0.55
3	11290032	316.22	8	3	130.34	1.40	-3.15	Y, 0 Violation	0.55
4	90785191	346.20	10	2	137.80	1.49	-3.54	Y, 0 Violation	0.55
5	145980140	472.44	10	4	151.98	1.34	-3.58	Y, 0 Violation	0.55
6	145658936	400.34	9	3	139.57	2.04	-3.93	Y, 0 Violation	0.55
7	166479754	424.49	6	3	104.06	4.15	-6.36	Y, 0 Violation	0.55
8	143180720	380.28	10	3	172.86	1.22	-3.30	Y, 0 Violation	0.11

9	5488919	330.25	8	2	119.34	1.79	-3.36	Y, 0 Violation	0.55
10	53946689	386.27	10	2	153.48	1.69	-3.23	Y, 0 Violation	0.55

Veber	Ghose	Egan	Muegge
Yes	No	Yes	Yes
No	Yes	No	No
Yes	Yes	Yes	Yes
Yes	Yes	No	Yes
No	Yes	No	No
Yes	Yes	No	Yes
Yes	Yes	Yes	No
No	Yes	No	No
Yes	Yes	Yes	Yes
No	Yes	No	No

Table 2a presents the physicochemical and drug-likeness properties of lead compounds from the Ellagic acid library tested against *T. rubrum's* ASADH (PDB: 4ZHS). The lead compounds in this library satisfy all the parameters of the Lipinski rules with zero violations. All of the compounds can be considered to have substantial intestinal absorption and favorable solubility in aqueous solutions, as their lipophilicity and Log S scores are within the acceptable range. Except for very few compounds, the TPSA values for the other lead compounds were found to be below permissible limits. Similarly, except for compound 8, the bioavailability value for all the compounds was 0.55, indicating optimal systemic circulation upon administration. For the additional filters that were used for the physicochemical analysis, the lead compounds in the ellagic acid library had negligible to comparable violations. Briefly, among all the compounds, Ghose had 1 violation, whereas Veber, Muegge, and Egan had 4, 5, and 6 violations, respectively.

Table 2b: Physicochemical Property Analyses of the IMB-XMA0038 Library (PDB: 4ZHS)

Sl.No	Compound ID	Mol.wt g/mol	HBA	HBD	TPSA (Å^2)	Log $P_{o/w}$ (Consensus)	Log S (ESOL)	Drug likeness: Y(Yes)/N(No) (Lipinski Rules)	Bio availability
1	7267137	426.29	11	6	191.03	1.36	-4.09	Y, 2 Violations	0.17
2	7655523	344.35	6	1	142.08	2.58	-4.34	Y, 0 Violation	0.55
3	7244049	344.35	6	1	142.08	2.56	-4.34	Y, 0 Violation	0.55
4	7655527	328.28	7	1	126.9	2.06	-3.85	Y, 0	0.55

					8			Violation	
5	2168077	282.25	5	0	93.60	1.51	-3.51	Y, 0 Violation	0.55
6	1356738	359.79	4	1	116.05	3.17	-4.94	Y, 0 Violation	0.55
7	678894	339.37	4	1	116.05	2.95	-4.65	Y, 0 Violation	0.55
8	4130759	318.24	8	1	132.30	0.53	-2.29	Y, 0 Violation	0.55
9	959022	345.40	4	1	144.29	3.10	-4.89	Y, 0 Violation	0.55
10	7686800	339.35	4	1	95.23	1.96	-3.46	Y, 0 Violation	0.55

Veber	Ghose	Egan	Muegge
No	Yes	No	No
No	Yes	No	Yes
No	Yes	No	Yes
Yes	Yes	Yes	Yes
Yes	Yes	Yes	Yes
Yes	Yes	Yes	Yes
Yes	Yes	Yes	Yes
Yes	Yes	No	Yes
No	Yes	No	Yes
Yes	Yes	Yes	Yes

Table 2b presents the physicochemical and drug-likeness properties of lead compounds from the IMB-XMA0038 library tested against *T. rubrum's* ASADH (PDB: 4ZHS). The lead compounds in this library satisfy all the parameters of Lipinski's rules except for two violations in the first compound. While all the compounds possess stronger intestinal absorption (log $P_{o/w}$ < 5), their systemic circulation upon consumption is also demonstrated, with an overall bioavailability score of 0.55. Furthermore, except for compound 1, and to an extent for 2, 3, and 9, the TPSA values for the remaining compounds were observed inside the expected limits. Likewise, in the case of predicting aqueous solubility, the Log S value of all the lead compounds was found to be either lower or negligibly higher than the optimal limit. For all the compounds, Ghose has zero violations, Muegge has 1 violation, Veber has 4 violations, and Egan has 5 violations.

Table 2c: Physicochemical Property Analyses of the 2-Chloro-3-Methoxy-1,4-Naphthoquinone Library (PDB: 4ZHS)

Sl.No	Compound ID	Mol.wt g/mol	HBA	HBD	TPSA ($Å^2$)	Log $P_{o/w}$ (Consensus)	Log S (ESOL)	Drug likeness: Y(Yes)/N(No	Bio availability

								) (Lipinski Rules)	
1	164517454	540.66	16	0	43.37	6.54	-7.17	Y, 1 Violation	0.85
2	11211153	378.76	5	0	77.51	3.05	-4.68	Y, 0 Violation	0.56
3	158303463	312.36	4	0	60.44	3.23	-3.82	Y, 0 Violation	0.85
4	20165701	264.70	3	0	43.37	2.99	-4.09	Y, 0 Violation	0.85
5	276680	264.66	4	0	60.44	2.27	-3.24	Y, 0 Violation	0.85
6	13887390	248.66	3	0	43.37	2.35	-3.39	Y, 0 Violation	0.85
7	164517453	322.64	7	0	43.37	3.36	-4.30	Y, 0 Violation	0.85
8	164517455	290.62	6	0	43.37	3.04	-4.10	Y, 0 Violation	0.85
9	275103	250.63	4	0	60.44	2.00	-3.10	Y, 0 Violation	0.85
10	54283595	292.76	3	0	43.37	3.54	-4.76	Y, 0 Violation	0.85

Veber	Ghose	Egan	Muegge
Yes	No	No	No
Yes	Yes	Yes	Yes
Yes	Yes	Yes	Yes
Yes	Yes	Yes	Yes
Yes	Yes	Yes	Yes

Yes	Yes	Yes	Yes
Yes	Yes	Yes	Yes
Yes	Yes	Yes	Yes
Yes	Yes	Yes	Yes
Yes	Yes	Yes	Yes

Table 2c presents the physicochemical and drug-likeness properties of lead compounds from the 2-chloro-3-methoxy-1,4-naphthoquinone library tested against *T. rubrum's* ASADH (PDB: 4ZHS). The lead compounds in this library satisfy all the parameters of Lipinski's rules except for one violation in the first compound. In terms of optimal systemic circulation, only compound 2 satisfied this criterion, with a bioavailability score of 0.56. All the compounds exhibited acceptable TPSA values and are also considered to have favorable lipophilicities, except for compound 1. As noted above, excluding the first compound, the aqueous solubility (Log S) value of the remaining lead compounds was found to be either lower or marginally higher than the optimal limit. For the additional filters that were used for the physicochemical analysis, all the lead compounds in this library had zero violations of the Veber filter and 1 violation of each of the Ghose, Egan, and Muegge filters.

Table 3a: Physicochemical Property Analyses of the Ellagic Acid Library (PDB: 6C85)

Sl. No	Compound ID	Mol. wt g/mol	HBA	HBD	TPSA (Å^2)	Log $P_{o/w}$ (Consensus)	Log S (ESOL)	Drug likeness: Y(Yes)/N(No) (Lipinski Rules)	Bio availability
1	11294619	482.44	8	2	119.34	4.18	-6.00	Y, 0 Violation	0.55
2	70681273	412.43	9	3	123.91	1.10	-2.96	Y, 0 Violation	0.55
3	5491816	330.25	8	2	119.34	1.83	-3.36	Y, 0 Violation	0.55
4	56676784	458.41	10	4	151.98	1.05	-3.27	Y, 0 Violation	0.55
5	91016455	448.34	10	4	167.64	2.45	-4.70	Y, 0 Violation	0.55
6	123263024	344.27	8	3	130.34	2.06	-3.72	Y, 0 Violation	0.55
7	91112913	360.23	10	3	156.64	1.35	-3.29	Y, 0 Violation	0.55
8	91157994	344.23	9	3	147.41	1.38	-3.08	Y, 0 Violation	0.55
9	53946689	386.27	10	2	153.48	1.69	-3.23	Y, 0 Violation	0.55
10	59184440	300.22	7	3	121.11	1.75	-3.39	Y, 0 Violation	0.55

Veber	Ghose	Egan	Muegge
Yes	No	Yes	Yes
Yes	Yes	Yes	Yes
Yes	Yes	Yes	Yes
No	Yes	No	No
No	Yes	No	No
Yes	Yes	Yes	Yes
No	Yes	No	No
No	Yes	No	Yes
No	Yes	No	No
Yes	Yes	Yes	Yes

Table 3a presents the physicochemical and drug-likeness properties of lead compounds from the Ellagic acid library docked against *B. dermatitidis's* ASADH (PDB: 6C85). As demonstrated by the physicochemical profile of T. rubrum's ASADH, the lead compounds in this library meet all of Lipinski's requirements and exhibit drug-like properties with zero violations. The overall values obtained for the bioavailability and lipophilicity parameters were within the acceptable range. With the exception of a few, the remaining compounds exhibited favorable aqueous solubilities (log S < -4) and TPSA scores (< 140 $Å^2$). In the case of the additional filters that were used for the physicochemical analysis, the lead compounds in the Ellagic acid library had negligible to comparable violations. Briefly, while the Ghose and Muegge filters resulted in 1 and 4 violations, respectively, Veber and Egan resulted in 5 violations, each among all the lead compounds.

Table 3b: Physicochemical Property Analyses of the IMB-XMA0038 Library (PDB: 6C85)

Sl. No	Compound ID	Mol. wt g/mol	HBA	HBD	TPSA ($Å^2$)	Log $P_{o/w}$ (Consensus)	Log S (ESOL)	Drug likeness: Y(Yes)/N(No) (Lipinski Rules)	Bio availability
1	12440425	335.38	5	1	121.81	1.94	-3.39	Y, 0 Violation	0.55
2	2104531	350.74	6	1	142.08	2.42	-4.15	Y, 0 Violation	0.55
3	7244049	344.35	6	1	142.08	2.56	-4.34	Y, 0 Violation	0.55
4	12549487	283.24	6	0	97.88	2.31	-3.77	Y, 0 Violation	0.55
5	2104545	340.70	7	1	155.22	1.99	-3.90	Y, 0 Violation	0.55
6	45809809	274.23	5	1	97.29	1.51	-3.14	Y, 0 Violation	0.55
7	2739411	300.2	7	1	126.9	1.24	-3.05	Y, 0	0.55

		3			8			Violation	
8	844311	304.73	3	1	74.92	3.16	-4.90	Y, 0 Violation	0.55
9	25818784	334.31	7	1	159.90	1.06	-3.01	Y, 0 Violation	0.55
10	7655523	344.35	6	1	142.08	2.58	-4.34	Y, 0 Violation	0.55

Veber	Ghose	Egan	Muegge
Yes	Yes	Yes	Yes
No	Yes	No	Yes
No	Yes	No	Yes
Yes	Yes	Yes	Yes
No	Yes	No	No
Yes	Yes	Yes	Yes
Yes	Yes	Yes	Yes
Yes	Yes	Yes	Yes
No	Yes	No	No
No	Yes	No	Yes

Table 3b presents the physicochemical and drug-likeness properties of lead compounds from the IMB-XMA0038 library docked against *B. dermatitidis's* ASADH (PDB: 6C85). The lead compounds in this library satisfy all the parameters of Lipinski's rules with zero violations. As described above, the lipophilicity of all the compounds was within the preferred limits, suggesting that they can be readily absorbed by the intestines. Similarly, the bioavailability score was within the ideal range, indicating that all compounds can have optimal systemic circulation upon administration. Except for very few compounds, the remaining compounds exhibited favorable aqueous solubilities (log S < -4) and TPSA scores (< 140 $Å^2$). For the additional filters that were used for the physicochemical analysis, the lead compounds in this library have zero violations of the Ghose filter, 2 violations of the Muegge filter, and 5 violations each of the Veber and Egan filters.

Table 3c: Physicochemical Property Analyses of the 2-Chloro-3-Methoxy-1,4-Naphthoquinone Library (PDB: 6C85)

Sl. No	Compound ID	Mol. wt g/mol	HBA	HBD	TPSA ($Å^2$)	Log $P_{o/w}$ (Consensus)	Log S (ESOL)	Drug likeness: Y(Yes)/N(No) (Lipinski Rules)	Bio availability
1	72792957	328.45	3	0	43.37	5.10	-5.75	Y, 0 Violation	0.85
2	19872801	258.31	3	0	43.37	3.31	-3.99	Y, 0 Violation	0.85

3	158303463	312.36	4	0	60.44	3.23	-3.82	Y, 0 Violation	0.85
4	164517454	540.66	16	0	43.37	6.54	-7.17	Y, 1 Violation	0.85
5	10945787	278.73	3	0	43.37	3.40	-4.32	Y, 0 Violation	0.85
6	19873044	272.34	3	0	43.37	3.67	-4.34	Y, 0 Violation	0.85
7	54283595	292.76	3	0	43.37	3.54	-4.76	Y, 0 Violation	0.85
8	11211153	378.76	5	0	77.51	3.05	-4.68	Y, 0 Violation	0.56
9	19872848	230.26	3	0	43.37	2.46	-3.22	Y, 0 Violation	0.85
10	19872838	244.29	3	0	43.37	2.81	-3.57	Y, 0 Violation	0.85

Veber	Ghose	Egan	Muegge
Yes	Yes	Yes	No
Yes	Yes	Yes	Yes
Yes	Yes	Yes	Yes
Yes	No	No	No
Yes	Yes	Yes	Yes
Yes	Yes	Yes	Yes
Yes	Yes	Yes	Yes
Yes	Yes	Yes	Yes
Yes	Yes	Yes	Yes
Yes	Yes	Yes	Yes

Table 3c presents the physicochemical and drug-likeness properties of lead compounds from the 2-chloro-3-methoxy-1,4-naphthoquinone library docked against *B. dermatitidis's* ASADH (PDB: 6C85). As observed with the other libraries, the lead compounds in this library also satisfy all the parameters of Lipinski's rules except for one violation (LogP > 5) in the fourth compound. With the exception of compound 8, the bioavailability range for the remaining compounds exceeded the optimal limit. Similarly, in terms of lipophilicity and Log S, all the compounds exhibited favorable intestinal absorption and favorable aqueous solubility, except for compounds 1 and 4. Apart from exhibiting the accepted TPSA values, all the lead compounds in this library have also shown zero violations of the Veber filter and negligible violations of the Ghose (1), Egan (1), and Muegge (2) filters.

Pharmacological Parameters and ADMET Properties

ADME studies are designed to investigate how a chemical is processed by a living organism. Toxicology tests are often a part of this process, yielding the acronym ADMET. A high-quality drug candidate

should not only have sufficient efficacy against the therapeutic target but also show appropriate ADMET properties at a therapeutic dose [30].

The following are the key parameters considered for the ADMET analysis. A Caco2 permeability > 0.90 cm/s indicates efficient human intestinal absorption of a drug, whereas compounds possessing an intestinal absorption (IA) of > 30% are considered promising drug candidates. Compounds with a skin permeability (SP) of "logKp > -2.5" are considered to have minimal penetration, whereas a value of "logBB > 0.3" is essential for crossing the blood-brain barrier (BBB). Additionally, values of "logBB < -1" are generally assumed to be poorly distributed in the brain. Similarly, central nervous system (CNS) permeability, "logPS > -2," indicates the ability of a compound to penetrate the CNS, whereas a permeability of "logPS < -3" suggests that it cannot penetrate. Assessment of cytochrome P450, an important detoxification enzyme that is found mainly in the liver, is essential because of its role in drug metabolism. In nature, they consist of many isoforms, such as CYP1A2 and CYP2C9, and compounds that can inhibit these enzymes may lead to drug-drug interactions or altered metabolism. Total clearance (TCL), which is often referred to as drug clearance, is related to the bioavailability of a given compound. It is used to measure the combined hepatic and renal clearance for the compound of interest and, hence, is considered vital in determining dosage concentrations. Organic cation transporter 2 (OCT2) is a renal uptake transporter that is primarily found in the kidneys and plays an important role in the disposition and renal clearance of drugs and endogenous compounds. Assessing a compound's potential to act as a substrate for renal OCT2 is critical for understanding its disposition and potential for renal excretion.

Toxicity studies were performed to investigate the safety profile of the candidate compounds. The positive results of the AMES test indicate that the compound is mutagenic and therefore may act as a carcinogen. Hepatotoxicity is the major safety concern for drug development, indicating the presence or absence of drug-induced liver injury. Skin sensitization predicts whether a compound can induce allergies in contact with the skin. The maximum recommended tolerated dose (MRTD) provides an estimate of the highest dose that can be administered (usually to animals in preclinical studies) without causing significant adverse effects. Hence, an MRTD greater than 0.477 log (mg/kg/day) is considered to have a good safety margin for the respective drug candidate.

In oral rat acute (LD50) and oral rat chronic (LOAEL) toxicity studies, the LD50 aims to determine the dose of a substance that is estimated to be lethal when it is administered to 50% of the test population, whereas the LOAEL estimates the lowest dose of a compound that results in an observed adverse effect in the test subjects. The lower the LD50 value, the more toxic the substance is considered to be. Conversely, a higher LD50 value indicates lower acute toxicity. The adverse effects can include physiological changes, biochemical alterations, or any other signs of toxicity that are considered detrimental to the health of the organism. Taken together, these evaluations lead to the selection of potential drug candidates with the best efficacy and safety profiles, allowing them to progress through the preclinical and clinical development stages.

Table 4a: Selected ADME Properties of the Ellagic Acid Library (PDB: 4ZHS)

Compound ID	Absorption			Distribution		Metabolism		Excretion	
	Caco2	IA	SP (log Kp)	BBB (log BB)	CNS (log PS)	CYP1A2 inhibitor	CYP2C9 inhibitor	TCL (log ml/min/kg)	Renal OCT2 substrate

11294619	-0.213	100	-2.735	-1.091	-2.996	No	Yes	0.550	No
91016455	0.129	100	-2.735	-1.542	-3.586	No	No	0.424	No
11290032	-0.075	96.333	-2.735	-1.245	-3.568	Yes	No	0.624	No
90785191	0.262	100	-2.735	-1.305	-3.822	No	No	0.500	No
145980140	0.198	73.657	-2.735	-1.083	-3.568	No	No	-0.013	No
145658936	0.396	100	-2.735	-1.440	-3.628	No	No	0.620	No
166479754	0.530	83.986	-2.736	-1.161	-2.748	No	Yes	0.046	No
143180720	-0.859	73.051	-2.735	-1.585	-3.544	No	No	0.715	No
5488919	0.157	100	-2.738	-1.029	-3.385	Yes	No	0.652	No
53946689	0.191	100	-2.735	-1.350	-3.857	No	No	0.879	No

Table 4a presents the ADME properties of lead compounds from the Ellagic acid library tested against *T. rubrum's* ASADH. Although the lead compounds in this library exhibit unfavorable permeability toward Caco2 cells, the majority of them exhibit substantial intestinal absorption with negligible skin penetration. The values of logBB for the BBB and logPS for CNS permeability are well below the permissible range, indicating that they cannot cross the BBB or can affect the CNS. For P450s, only compounds 3 and 9 inhibited CYP1A2, whereas compounds 1 and 7 inhibited CYP2C9. Likewise, among the top-ranked compounds, compound 10 has exhibited a faster clearance rate. For the renal OCT2 substrate, none of the lead compounds acted as substrates.

Table 4b: Toxicity Predictions for the Ellagic Acid Library (PDB: 4ZHS)

Compound ID	AMES toxicity	Hepato-toxicity	Skin Sensitization	Maximum tolerated dose	Oral Rat Acute Toxicity (LD50)	Oral Rat Chronic Toxicity (LOAEL)
11294619	Yes	No	No	0.339	2.533	2.304
91016455	No	No	No	0.534	2.504	3.122
11290032	Yes	No	No	0.582	2.373	2.232
90785191	No	No	No	0.080	2.204	2.654
145980140	No	No	No	0.130	1.979	3.277
145658936	No	Yes	No	0.532	2.378	2.205
166479754	No	No	No	-0.041	2.171	2.117
143180720	No	Yes	No	0.930	2.493	3.149

5488919	Yes	No	No	0.240	2.174	2.165
53946689	No	No	No	0.117	2.215	2.607

Table 4b presents the toxicity predictions of lead compounds from the Ellagic acid library against *T. rubrum's* ASADH. Except for a very few compounds, most of them have shown negative effects for both AMES and hepatotoxicity. In addition, none of the compounds can induce allergies when exposed to the skin. In terms of MRTD, with the exception of compounds 4, 5, 7, and 10, the remaining compounds are considered to have moderate to high tolerance, indicating that adverse effects can be observed only at relatively high doses. For the LD50, among the lead compounds, 1, 2, 3, 6, and 8 are considered to have lower acute toxicity levels. Furthermore, the chronic toxicity (LOAEL) levels of compounds 2, 4, 5, 8, and 10 suggest that harmful effects occur only at reasonably high doses.

Table 4c: Selected ADME Properties of the IMB-XMA0038 Library (PDB: 4ZHS)

Compound ID	Absorption			Distribution		Metabolism		Excretion	
	Caco2	IA	SP (log Kp)	BBB (log BB)	CNS (log PS)	CYP1A2 inhibitor	CYP2C9 inhibitor	TCL (log ml/min/kg)	Renal OCT2 substrate
7267137	1.639	89.253	-2.735	-1.052	-2.598	Yes	Yes	0.100	No
7655523	0.335	90.010	-2.759	-0.695	-2.099	Yes	Yes	-0.145	No
7244049	0.335	90.010	-2.759	-0.695	-2.099	Yes	Yes	-0.037	No
7655527	0.616	88.293	-2.761	-0.884	-2.381	Yes	Yes	0.177	No
2168077	1.248	95.511	-2.659	-0.749	-2.365	Yes	Yes	0.220	No
1356738	1.166	87.799	-2.707	-0.743	-1.916	Yes	Yes	0.151	No
678894	0.602	90.189	-2.745	-0.340	-1.757	Yes	Yes	0.227	No
4130759	0.027	74.912	-2.746	-0.508	-2.906	No	No	0.094	No
959022	0.564	88.475	-2.759	-0.556	-1.792	Yes	Yes	0.253	No
7686800	1.120	97.269	-2.749	-0.426	-2.184	Yes	Yes	0.256	No

Table 4c presents the ADME properties of lead compounds from the IMB-XMA0038 library tested against *T. rubrum's* ASADH. The lead compounds 1, 5, 6 and 10 exhibited favorable permeability toward Caco2 cells. Similarly, all the compounds possess substantial intestinal absorption with negligible skin penetration. Though no compounds have shown the tendency to cross the BBB, few among them (compounds 6, 7 and 9) were found to permeate the CNS. For P450s, most of the compounds inhibited CYP1A2 and CYP2C9. Except for compounds 2 and 3, the remaining compounds

exhibited relatively faster clearance. For the renal OCT2 substrate, none of the lead compounds acted as substrates.

Table 4d: Toxicity Predictions for the IMB-XMA0038 Library (PDB: 4ZHS)

Compound ID	AMES toxicity	Hepato-toxicity	Skin Sensitization	Maximum tolerated dose	Oral Rat Acute Toxicity (LD50)	Oral Rat Chronic Toxicity (LOAEL)
7267137	No	Yes	No	0.868	2.378	1.180
7655523	Yes	Yes	No	-0.137	2.888	1.249
7244049	Yes	Yes	No	-0.137	2.888	1.249
7655527	Yes	Yes	No	0.077	2.917	0.943
2168077	Yes	Yes	No	0.223	2.332	1.511
1356738	Yes	Yes	No	0.507	2.794	1.098
678894	Yes	Yes	No	-0.288	2.982	1.651
4130759	Yes	Yes	No	0.382	2.497	0.932
959022	Yes	No	No	-0.283	3.084	1.465
7686800	Yes	Yes	No	-0.164	2.481	1.702

Table 4d presents the toxicity predictions of lead compounds from the IMB-XMA0038 library tested against *T. rubrum's* ASADH. Although no compounds can cause allergies to the skin, the majority of them are positive for AMES and hepatotoxicity. In terms of MRTD, compounds 1, 6, and 8 are considered to have favorable safety margins, whereas, for the LD50, the majority of the compounds are considered to have lower acute toxicity levels. Furthermore, the chronic toxicity (LOAEL) levels of compounds 2, 3, 5, 7, 9, and 10 suggest that harmful effects occur only at reasonably high doses.

Table 4e: Selected ADME Properties of the 2-Chloro-3-Methoxy-1,4-Naphthoquinone Library (PDB: 4ZHS)

Cmp ID	Absorption			Distribution		Metabolism		Excretion	
	Caco2	IA	SP (log Kp)	BBB (log BB)	CNS (log PS)	CYP1A2 inhibitor	CYP2C9 inhibitor	TCL (log ml/min/kg)	Renal OCT2 substrate
164517454	1.248	82.582	-2.680	0.545	-3.285	No	No	0.640	No
11211153	1.371	99.825	-2.739	-0.545	-1.985	Yes	Yes	0.431	No
158303463	1.410	96.615	-2.842	-0.371	-2.196	Yes	No	0.323	No
20165701	1.382	96.612	-2.650	0.309	-1.935	Yes	Yes	0.309	No
276680	1.316	97.190	-2.763	0.045	-2.840	Yes	No	0.160	No

13887390	1.338	96.340	-2.638	0.344	-2.311	Yes	Yes	0.155	No
164517453	1.421	91.495	-2.401	0.588	-2.531	No	No	0.391	No
164517455	1.393	92.309	-2.357	0.635	-2.333	Yes	No	0.298	No
275103	1.291	97.364	-2.756	0.078	-2.850	Yes	No	0.130	No
54283595	1.452	95.157	-2.585	0.030	-1.847	Yes	No	0.175	Yes

Table 4e presents the ADME properties of lead compounds from the 2-chloro-3-methoxy-1,4-naphthoquinone library tested against *T. rubrum's* ASADH. All the lead compounds exhibited favorable permeability toward Caco2 cells and substantial intestinal absorption. Except for compounds 7 and 8, most of them cannot penetrate the skin. Likewise, except for a few compounds (1, 6. 7, and 8 for logBB, and 2, 4, and 10 for logPS), the remaining compounds can neither cross the BBB nor permeate the CNS. With respect to P450s, almost all the compounds inhibited CYP1A2 except compounds 1 and 7, whereas excluding compounds 2, 4, and 6, the remaining compounds did not inhibit CYP2C9. The values obtained for the TCL parameter have shown that few compounds may exhibit faster clearance than others. With the exception of compound 10, the rest of the compounds cannot act as substrates for renal OCT2.

Table 4f: Toxicity Predictions for the 2-Chloro-3-Methoxy-1,4-Naphthoquinone Library (PDB: 4ZHS)

Compound ID	AMES toxicity	Hepato-toxicity	Skin Sensitization	Maximum tolerated dose	Oral Rat Acute Toxicity (LD50)	Oral Rat Chronic Toxicity (LOAEL)
164517454	No	Yes	No	-0.139	3.120	0.472
11211153	No	No	No	0.697	2.395	1.708
158303463	No	Yes	No	0.824	1.857	2.128
20165701	No	Yes	No	0.919	2.373	1.941
276680	Yes	No	No	0.991	2.527	1.243
13887390	Yes	Yes	No	0.513	2.048	1.864
164517453	No	No	No	0.361	2.621	1.325
164517455	No	No	No	0.453	2.457	1.411
275103	Yes	No	No	0.958	2.496	1.209
54283595	No	Yes	No	0.540	2.374	1.976

Table 4f presents the toxicity predictions of lead compounds from the 2-chloro-3-methoxy-1,4-naphthoquinone library tested against *T. rubrum's* ASADH. The majority of the compounds exhibited negative AMES and hepatotoxicity. Additionally, no compounds can induce allergies in contact with the skin. In terms of MRTD, with the exception of compound 1, all of these compounds can be considered to have good safety margins. For the LD50, among the lead compounds, 1, 5, 7, 8, and 9 are considered to

have lower acute toxicity levels. Furthermore, the chronic toxicity (LOAEL) levels of compounds 2, 3, 4, 6, and 10 suggest that harmful effects occur only at relatively higher doses.

Table 5a: Selected ADME Properties of the Ellagic Acid Library (PDB: 6C85)

Cmp ID	Absorption			Distribution		Metabolism		Excretion	
	Caco2	IA	SP (log Kp)	BBB (log BB)	CNS (log PS)	CYP1A2 inhibitor	CYP2C9 inhibitor	TCL (log ml/min/kg)	Renal OCT2 substrate
11294619	-0.213	100	-2.735	-1.091	-2.996	No	Yes	0.550	No
70681273	1.090	77.528	-2.823	-1.353	-3.425	No	No	0.817	No
5491816	0.134	100	-2.736	-0.817	-3.458	Yes	No	0.684	No
56676784	0.263	78.534	-2.735	-1.129	-3.569	No	No	-0.011	No
91016455	0.129	100	-2.735	-1.542	-3.586	No	No	0.424	No
123263024	-0.121	100	-2.735	-1.359	-3.345	Yes	No	0.628	No
91112913	0.254	98.688	-2.735	-1.724	-3.986	No	No	0.709	No
91157994	0.288	100	-2.735	-1.504	-3.708	Yes	No	0.685	No
53946689	0.191	100	-2.735	-1.350	-3.857	No	No	0.879	No
59184440	-0.004	99.99	-2.735	-1.161	-2.363	Yes	No	0.573	No

Table 5a presents the ADME properties of lead compounds from the Ellagic acid library tested against *B. dermatitidis's* ASADH. Although the lead compounds exhibited unfavorable permeability toward Caco2 cells (< 0.90 cm/s), still all of the compounds possessed substantial intestinal absorption with no skin penetration. The values obtained for logBB and logPS have shown that none of them can cross the BBB or permeate the CNS. For P450s, only compounds 3, 6, 8, and 10 inhibited CYP1A2, whereas compound 1 inhibited CYP2C9. Similarly, among the top-ranked compounds, compound 9 has demonstrated faster clearance, whereas compound 4 has shown slower clearance. The renal OCT2 substrate shows favorable results for all the compounds, as none of them acted as substrates.

Table 5b: Toxicity Predictions for the Ellagic Acid Library (PDB: 6C85)

Compound ID	AMES toxicity	Hepato-toxicity	Skin Sensitization	Maximum tolerated dose	Oral Rat Acute Toxicity (LD50)	Oral Rat Chronic Toxicity (LOAEL)
11294619	Yes	No	No	0.339	2.533	2.304
70681273	No	No	No	0.227	2.638	3.206
5491816	Yes	No	No	0.288	2.172	1.861
56676784	No	No	No	-0.486	2.071	3.037
91016455	No	No	No	0.534	2.504	3.122
123263024	No	No	No	0.533	2.384	2.167
91112913	No	No	No	0.506	2.370	2.558
91157994	No	No	No	0.556	2.364	2.400
53946689	No	No	No	0.117	2.215	2.607
59184440	Yes	No	No	0.627	2.397	2.120

Table 5b presents the toxicity predictions of lead compounds from the Ellagic acid library tested against *B. dermatitidis's* ASADH. While a very few compounds have shown positive AMES toxicity, none have exhibited hepatotoxic effects and cannot induce any allergies upon exposure to the skin. With the exception of a few, most of the compounds have shown moderate to high tolerance in terms of MRTD. Both the acute and chronic toxicity profiles have shown that all the compounds presented with higher LD50 and LOAEL values, indicating lower acute toxicity and thus proving that harmful effects can occur only at reasonably high doses.

Table 5c: Selected ADME Properties of the IMB-XMA0038 Library (PDB: 6C85)

Cmp ID	Absorption			Distribution		Metabolism		Excretion	
	Caco2	IA	SP (log Kp)	BBB (log BB)	CNS (log PS)	CYP1A2 inhibitor	CYP2C9 inhibitor	TCL (log ml/min/kg)	Renal OCT2 substrate
12440425	1.110	95.573	-2.875	-0.454	-2.196	No	No	0.053	Yes
2104531	1.293	90.070	-2.730	-1.137	-2.300	Yes	Yes	0.144	No
7244049	0.335	90.010	-	-	-	Yes	Yes	-0.037	No

			2.759	0.695	2.099				
12549487	0.915	100	-2.633	-0.783	-2.140	Yes	Yes	0.297	No
2104545	0.365	88.860	-2.771	-1.215	-3.021	Yes	No	0.138	No
45809809	0.515	97.849	-2.825	-0.480	-2.365	Yes	No	0.425	No
2739411	0.522	97.317	-2.755	-1.025	-2.525	Yes	Yes	0.179	No
844311	0.493	90.490	-2.712	-0.279	-1.896	Yes	Yes	0.122	No
25818784	0.582	79.727	-2.747	-1.079	-2.700	Yes	No	0.106	No
7655523	0.335	90.010	-2.759	-0.695	-2.099	Yes	Yes	-0.145	No

Table 5c presents the ADME properties of lead compounds from the IMB-XMA0038 library tested against *B. dermatitidis's* ASADH. Among this list, only compounds 1, 2, and 4 exhibited favorable permeability toward Caco2 cells. However, all the compounds have demonstrated substantial intestinal absorption with negligible skin penetration. The values obtained for logBB and logPS have shown that while no compounds could breach the BBB, except for compound 8, none of them can permeate the CNS as well. Concerning P450s, except for a few, almost all the other compounds inhibited CYP1A2 and CYP2C9. The values obtained for the TCL parameter have suggested that all the compounds may exhibit relatively slower clearance. For the renal OCT2 substrate, none of the lead compounds acted as substrates except for compound 1.

Table 5d: Toxicity Predictions for the IMB-XMA0038 Library (PDB: 6C85)

Compound ID	AMES toxicity	Hepato-toxicity	Skin Sensitization	Maximum tolerated dose	Oral Rat Acute Toxicity (LD50)	Oral Rat Chronic Toxicity (LOAEL)
12440425	Yes	No	No	-0.694	2.330	1.496
2104531	Yes	Yes	No	0.653	2.746	1.027
7244049	Yes	Yes	No	-0.137	2.888	1.249
12549487	Yes	Yes	No	0.190	2.798	1.768
2104545	Yes	Yes	No	0.338	2.793	1.039
45809809	Yes	No	No	0.027	2.754	1.530
2739411	Yes	Yes	No	0.155	2.913	1.932
844311	Yes	No	No	0.172	2.949	1.733
25818784	Yes	Yes	No	0.201	2.558	0.871
7655523	Yes	Yes	No	-0.137	2.888	1.249

Table 5d presents the toxicity predictions of lead compounds from the IMB-XMA0038 library tested against *B. dermatitidis's* ASADH. Although none of the compounds have been found to cause any

allergies to the skin, all the compounds exhibited positive AMES and hepatotoxicity (excluding compounds 1, 6, and 8). In terms of MRTD, except for compound 2, the rest of them possessed only moderate tolerance levels. As for the acute and chronic toxicity, all the compounds are presented with higher LD50 and LOAEL values, suggesting lower acute toxicity and further confirming that harmful effects are expected to occur only at relatively higher doses.

Table 5e: Selected ADME Properties of the 2-Chloro-3-Methoxy-1,4-Naphthoquinone Library (PDB: 6C85)

Cmp ID	Absorption			Distribution		Metabolism		Excretion	
	Caco2	IA	SP (log Kp)	BBB (log BB)	CNS (log PS)	CYP1A2 inhibitor	CYP2C9 inhibitor	TCL (log ml/min/kg)	Renal OCT2 substrate
72792957	1.579	93.537	-2.571	-0.002	-1.628	Yes	Yes	1.563	No
19872801	1.390	95.261	-2.443	0.207	-1.907	Yes	No	0.314	No
158303463	1.410	96.615	-2.842	-0.371	-2.196	Yes	No	0.323	No
164517454	1.248	82.582	-2.680	0.545	-3.285	No	No	0.640	No
10945787	1.407	95.154	-2.652	0.255	-2.067	Yes	Yes	0.385	No
19873044	1.413	94.911	-2.452	0.166	-1.846	Yes	No	0.330	No
54283595	1.452	95.157	-2.585	0.030	-1.847	Yes	No	0.175	Yes
11211153	1.371	99.825	-2.739	-0.545	-1.985	Yes	Yes	0.431	No
19872848	1.345	96.592	-2.484	0.222	-1.836	Yes	No	0.232	No
19872838	1.362	95.897	-2.513	0.285	-2.099	Yes	No	0.269	No

Table 5e presents the ADME properties of lead compounds from the 2-chloro-3-methoxy-1,4-naphthoquinone library tested against *B. dermatitidis's* ASADH. All the lead compounds exhibited favorable permeability toward Caco2 cells and substantial intestinal absorption. Incidentally, few compounds in this library are susceptible to skin permeability (compounds 2, 6, and 9). However, the distribution profile showed a mixed trait, where the majority of the compounds cannot cross the BBB; on the other hand, several compounds have shown the tendency to permeate into the CNS. With respect to P450s, all the compounds inhibited CYP1A2 except compound 4, whereas only compounds 1, 5, and 8 inhibited CYP2C9. The TCL values suggest that the compounds' clearance rates can range from moderately faster to slower. Except for compound 1, none of the top-ranked compounds acted as substrates for renal OCT2.

Table 5f: Toxicity Predictions for the 2-Chloro-3-Methoxy-1,4-Naphthoquinone Library (PDB: 6C85)

Compound ID	AMES toxicity	Hepato-toxicity	Skin Sensitization	Maximum tolerated dose	Oral Rat Acute Toxicity (LD50)	Oral Rat Chronic Toxicity (LOAEL)
72792957	No	No	Yes	0.895	1.828	2.758
19872801	No	No	No	0.905	1.754	2.386
158303463	No	Yes	No	0.824	1.857	2.128
164517454	No	Yes	No	-0.139	3.120	0.472
10945787	No	No	No	0.849	2.478	2.035
19873044	No	No	No	0.902	1.765	2.461
54283595	No	Yes	No	0.540	2.374	1.976
11211153	No	No	No	0.697	2.395	1.708
19872848	No	No	No	0.936	1.698	2.311
19872838	No	Yes	No	0.925	1.767	2.215

Table 5f presents the toxicity predictions of lead compounds from the 2-chloro-3-methoxy-1,4-naphthoquinone library tested against *B. dermatitidis's* ASADH. AMES toxicity has favorable results for all the compounds, and no compounds except compound 1 can induce allergies when they are in contact with the skin. All the compounds exhibited good safety concerns for drug development, indicating the absence of drug-induced liver injury, except for compounds 3, 4, 7, and 10. In terms of MRTD, almost all the compounds except compound 4 are considered to have good safety margins by possessing higher tolerance levels. Furthermore, the acute and chronic toxicity profiles have shown that all the compounds exhibited relatively higher LD50 and LOAEL values, suggesting minimal acute toxicity, with harmful effects most likely to occur only at high doses.

Discussion

Understanding the physiopathology of dermatophytosis is crucial to understanding fungal activity, which is essential for creating better therapeutic options. Epidemiological research has shown that *T. rubrum* is the leading cause of human dermatophytosis worldwide [31]. On the other hand, *B. dermatitidis* infection is uncommon, and unfortunately, there are no known practical measures for the prevention of blastomycosis. Awareness of the disease by both the public and health care providers is the key to early diagnosis [32]. Despite the periodic identification and development of new antifungal agents to treat fungal infections, many existing drugs inhibit only fungal growth (acting as fungistatic) rather than killing the entire pathogen (i.e., fungicidal). Moreover, many of these compounds also show significant toxicity in mammalian species [33]. Therefore, to overcome this limitation, researchers are exploring potential drug targets in the amino acid biosynthesis pathways found in various fungal pathogens [34].

The aspartate biosynthetic pathway is one such pathway that consists of several key enzymes and facilitates the biosynthesis of essential amino acids (e.g., threonine, isoleucine, and methionine) in their hosts. Due to their importance in this pathway, where they catalyze the second committed step, ASADH has emerged as an attractive drug target for the design and development of new antifungal agents. Taken together, the current study employed various computational techniques to identify and assess potential small-molecule inhibitors for ASADH from *T. rubrum* and *B. dermatitidis*. The study was initiated by

screening potential lead compounds as evidenced by their antifungal activities reported against these pathogens [19–24]. Ellagic acid, a naturally occurring substance, has demonstrated promising results *in silico*, outperforming existing drugs. Another compound, IMB-XMA0038, exhibited potent inhibitory effects at remarkably low levels against drug-resistant bacteria. Notably, IMB-XMA0038 is considered a robust inhibitor of ASADH, a crucial enzyme in fungal metabolism. The third lead compound, 2-chloro-3-methoxy-1,4-naphthoquinone, has also emerged as an effective ASADH inhibitor across various pathogenic fungi, including *Cryptococcus neoformans*, *Candida albicans*, *Aspergillus fumigatus*, and *B. dermatitidis*.

Hence, small molecule libraries were constructed using these three lead compounds, following which, virtual screening docking was performed against *T. rubrum* and *B. dermatitidis's* ASADH. The docking simulations, facilitated by PyRx, showed that the binding energies observed for the higher-ranked compounds from the three libraries were significantly greater when compared to several known existing antifungal drugs. Additionally, the docking results have also revealed that a few higher-ranked compounds, such as 11294619, 91016455, and 53946689 from the Ellagic acid library; 7244049 from the IMB-XMA0038 library; 164517454, 11211153, 158303463, and 54283595 from the 2-chloro-3-methoxy-1,4-naphthoquinone library, exhibited affinities for both *T. rubrum* and *B. dermatitidis's* ASADH, however, with varying binding energies (Table 1a and 1b).

Furthermore, the higher-ranked compounds in Tables 1a and 1b were subjected to in-depth physicochemical analysis. The results clearly showed that all the compounds were not only found to abide by Lipinski's parameters but also demonstrated their conformity to drug-likeness criteria (Table 2a-2c and Table 3a-3c). Following this, a comprehensive evaluation of ADME properties was performed using pkCSM. The absorption profile for the Caco2 permeability has revealed that among the three libraries, only in the 2-Chloro-3-Methoxy-1,4-Naphthoquinone library, all the compounds possessed the required threshold of > 0.90 cm/s permeability. On the contrary, all compounds from the three libraries have exceeded the expected 30% threshold for intestinal absorption, confirming their readiness for absorption through the gastrointestinal tract. The distribution characteristics comprising the BBB and CNS permeability indicated that no compounds from the three libraries showed a tendency to penetrate either the BBB or CNS. However, the metabolism profiles represented by the P450 enzymes showed that the three libraries of compounds exhibited a mixed trait where few compounds inhibited both CYP1A2 and CYP2C9. The excretion profile, which included the TCL and renal OCT2 characteristics, revealed that, in addition to displaying efficient clearance levels, most compounds in the three libraries could not act as renal OCT2 substrates, thereby lowering the risk of enhanced renal clearance.

When it comes to toxicity, predicting key properties of lead compounds can provide valuable insights into their safety characteristics. Very few compounds in each library displayed a positive effect on mutagenic (AMES) and liver toxicity, while the majority of the other compounds did not exhibit these toxicities or can induce any allergenic reactions when exposed to the skin. The safety margins were assessed using parameters like MRTD, LD50, and LOAEL. The analysis of MRTD scores showed that most compounds from the three libraries presented higher to moderate tolerance levels. Similarly, the scores for acute (LD50) and chronic (LOAEL) oral toxicity values indicated that all three libraries demonstrated lower toxicity levels, further confirming their safety margins in the theoretical model. To summarize, the potential compounds with stronger binding affinities and favorable pharmacokinetic profiles identified from the three libraries can undergo further *in vitro* and *in vivo* validation studies. This

will help evaluate their efficacy, safety, and potency as antifungal agents that can be used to treat infections caused by *T. rubrum* and *B. dermatophytosis*.

Conclusion

In conclusion, this study has highlighted the systematic approach employed in drug discovery, which integrates virtual screening, molecular docking, and ADMET evaluations to streamline the early-stage identification of potential drug candidates. By disrupting the biosynthesis of essential amino acids in fungi, ASADH inhibitors can constitute a novel class of antifungal drugs with broad-spectrum efficacy against diverse pathogenic fungi. The identified compounds present opportunities for lead optimization, with the potential for structural modifications to increase effectiveness and minimize side effects. Furthermore, combination therapies, understanding resistance mechanisms, and detailed pharmacokinetic and toxicological studies are imperative for the successful translation of these findings into clinical treatments.

Acknowledgement

The authors would like to acknowledge the support offered by Dr. Monika Chauhan, PhD, Program Director and Dr. Shashank Taxak, CEO, at Quick IsCool for providing essential resources and creating an environment conducive to research.

Author Contributions

Conceptualization: LK; Software: SN, SS, OAMD; Investigation: SN, SS, OAMD; Methodology: SN, SS, OAMD; Formal Analysis: SN; Writing - Original Draft Preparation: SN, SS, OAMD; Writing - Review & Editing: SN, LK; Supervision: LK.

Conflict of Interest

The authors have no competing interests to declare.

Funding

No funding was received for this study.

Data Availability

The data supporting the findings of this study are available within the manuscript.

Ethics Statement

Not applicable.

References

1. Rita A., “A One Health Approach to Combating Fungal Disease: Forward-Reaching Recommendations for Raising Awareness”. https://asm.org/Articles/2019/September/A-One-Health-Approach-to-Combating-Fungal-Disease
2. Bongomin F., Gago S., Oladele R.O., Denning D.W., “Global and Multi-National Prevalence of Fungal Diseases—Estimate Precision”, J Fungi, October 2017, 3 (4), 57.

3. de Hoog G.S., Dukik K., Monod M., Packeu A., Stubbe D., Hendrickx M., Kupsch C., Stielow J.B., Freeke J., Göker M., Rezaei-Matehkolaei A., Mirhendi H., Gräser Y., "Toward a Novel Multilocus Phylogenetic Taxonomy for the Dermatophytes", Mycopathologia, October 2016, 182 (1-2), 5–31.
4. Makimura K., Tamura Y., Mochizuki T., Hasegawa A., Tajiri Y., Hanazawa R., Uchida K., Saito H., Yamaguchi H., "Phylogenetic Classification and Species Identification of Dermatophyte Strains Based on DNA Sequences of Nuclear Ribosomal Internal Transcribed Spacer 1 Regions", J Clin Microbiol, April 1999, 37 (4), 920–4.
5. Dahl M.V., Grando S.A., "Chronic dermatophytosis: what is special about Trichophyton rubrum?", Adv Dermatol, January 1994, 9, 97–111.
6. Lee W.J., Kim S.L., Jang Y.H., Lee S.J., Kim D.W., Bang Y.J., Jun J.B., "Increasing Prevalence of Trichophyton rubrum Identified through an Analysis of 115,846 Cases over the Last 37 Years", J Korean Med Sci, April 2015, 30 (5), 639.
7. Erick M.H., Gabriela M.C., Claudia E.F.V., Rigoberto H.C., Roberto A., Rodolfo P.A., Carmen R.C., "Main Phenotypic Virulence Factors Identified in *Trichophyton rubrum*", Journal of Biological Regulators and Homeostatic Agents, May 2023, 37 (5), 2345–56.
8. Henry R., "Etymologia: Blastomycosis", Emerg Infect Dis, November 2014, 20 (11), 1794.
9. Sterkel A.K., Mettelman R., Wüthrich M., Klein B.S., "The Unappreciated Intracellular Lifestyle of Blastomyces dermatitidis", J Immunol, January 2015, 194 (4), 1796–805.
10. McBride J.A., Gauthier G.M., Klein B.S., "Turning on virulence: Mechanisms that underpin the morphologic transition and pathogenicity of Blastomyces", Virulence, August 2018, 10 (1), 801–9.
11. Abrahamian F.M., Goldstein E.J., "Microbiology of animal bite wound infections", Clin Microbiol Rev, April 2011, 24 (2), 231–46.
12. Baer S.L., Pappas P.G., "Hematogenously disseminated fungal infections", Clinical Mycology, November 2009, 609–22.
13. Dahal G.P., Viola R.E., "Structural insights into inhibitor binding to a fungal ortholog of aspartate semialdehyde dehydrogenase", Biochem Biophys Res Commun, September 2018, 503 (4), 2848–54.
14. Teakel S.L., Fairman J.W., Muruthi M.M., Abendroth J., Dranow D.M., Lorimer D.D., Myler P.J., Edwards T.E., Forwood J.K., "Structural characterization of aspartate-semialdehyde dehydrogenase from Pseudomonas aeruginosa and Neisseria gonorrhoeae", Sci Rep, August 2022, 12 (1), 1–11.
15. Li Q., Mu Z., Zhao R., Dahal G., Viola R.E., Liu T., Jin Q., Cui S., "Structural Insights into the Tetrameric State of Aspartate-β-semialdehyde Dehydrogenases from Fungal Species", Sci Rep, February 2016, 6 (1), 1–13.
16. McBride J.A., Gauthier G.M., Klein B.S., "Clinical Manifestations and Treatment of Blastomycosis", Clin Chest Med, September 2017, 38 (3), 435–49.
17. Dahal G.P., Launder D., McKeone K.M.M., Hunter J.P., Conti H.R., Viola R.E., "Aspartate semialdehyde dehydrogenase inhibition suppresses the growth of the pathogenic fungus Candida albicans", Drug Development Research, May 2020, 81 (6), 736–44.
18. Lang G., Buchbauer G., "A review on recent research results (2008-2010) on essential oils as antimicrobials and antifungals. A review", Flavour Fragr J, August 2011, 27 (1), 13–39.
19. Neves A.M., Fontenelle R.O., Lopes F.S., Mendes J.D., Rodrigues A.L., Marinho M.M., Marinho E.S., Morais S.M., "Phenolic profile, antioxidant and antifungal activity of extracts from four medicinal plants of the Anacardiaceae family", Res Soc Dev, July 2021, 10 (8), e44510817421.

20. Li Z.J., Guo X., Dawuti G., Aibai S., "Antifungal Activity of Ellagic Acid In Vitro and In Vivo", Phytotherapy Res, April 2015, 29(7), 1019–25.
21. Xiao Wang., Ruifang Yang., Sihan Liu., Yan Guan., Chunling Xiao., Chuanyou Li., Jianzho Meng., Yu Pang., Yishuang Liu., "IMB-XMA0038, a new inhibitor targeting aspartate-semialdehyde dehydrogenase of *Mycobacterium tuberculosis*", Emerg Microbes Infect, December 2021, 10 (1), 2291–99.
22. White T.C., Findley K., Dawson T.L. Jr., Scheynius A., Boekhout T., Cuomo C.A., Xu J., Saunders C.W., "Fungi on the skin: dermatophytes and Malassezia", Cold Spring Harb Perspect Med, August 2014, 4 (8), a019802.
23. Goughenour K.D., Rappleye C.A., "Antifungal therapeutics for dimorphic fungal pathogens", Virulence, February 2017, 8 (2), 211–221.
24. Dahal G.P., Viola R.E., "A Fragment Library Screening Approach to Identify Selective Inhibitors against an Essential Fungal Enzyme", SLAS Discov, July 2018, 23 (6), 520–531.
25. Dallakyan S., Olson A.J., "Small-molecule library screening by docking with PyRx", Methods Mol. Biol, January 2015, 1263, 243–250.
26. Goddard T.D., Huang C.C., Meng E.C., Pettersen E.F., Couch G.S., Morris J.H., Ferrin T.E., "UCSF ChimeraX: Meeting modern challenges in visualization and analysis", Protein Sci, January 2018, 27 (1), 14–25.
27. Dassault Systèmes BIOVIA, Discovery Studio Visualizer, v20.1.0.19295, San Diego: Dassault Systèmes 2020.
28. Daina A., Michielin O., Zoete V., "SwissADME: a free web tool to evaluate pharmacokinetics, drug-likeness and medicinal chemistry friendliness of small molecules", Scientific Reports, March 2017, 7, 42717.
29. Pires D.E.V., Blundell T.L., Ascher D.B., "pkCSM: Predicting Small-Molecule Pharmacokinetic and Toxicity Properties Using Graph-Based Signatures", Journal of Medicinal Chemistry, April 2015, 58 (9), 4066–72.
30. Clark A.M., Dole K., Coulon-Spektor A., McNutt A., Grass G., Freundlich J.S., Reynolds R.C., Ekins S., "Open Source Bayesian Models. 1. Application to ADME/Tox and Drug Discovery Datasets", J Chem Inf Model, June 2015, 55 (6), 1231–45.
31. Kanimozhi A.M., Aranganathan V., Rose J.C., "Identification and In Silico Analysis of Interaction of Active Compounds in Pimpinella anisum with Trichophyton rubrum Aspartate-B-Semialdehyde Dehydrogenase and Sialidase", Indian Journal of Pharmaceutical Sciences, May 2024, 86 (3), 872–81.
32. Pai V., Ganavalli A., Kikkeri N.N., "Antifungal Resistance in Dermatology", Indian J Dermatol, September-October 2018, 63 (5), 361–68.
33. Saccente M., Woods G.L., "Clinical and laboratory update on blastomycosis", Clin Microbiol Rev, April 2010, 23 (2), 367–81.
34. Kauffman C.A., Carver P.L., "Update on echinocandin antifungals", Semin Respir Crit Care Med, April 2008, 29 (2), 211–9.